**Table 1. SURFACE convergence parameters estimated using the MCC tree, as well as 100 trees from the Bayesian posterior probability distribution of *Anolis* phylogeny.**

| | MCC phylogeny | Mean (SD) for 100 sampled phylogenies |
|---|---|---|
| Adaptive peak shifts | 29 | 25.7 (2.1) |
| Convergent adaptive peak shifts | 22 | 20.2 (1.9) |
| Adaptive peaks | 15 | 12.7 (1.4) |
| Convergent adaptive peaks | 8 | 7.2 (0.97) |
| Convergence fraction (convergent peak shifts/total peak shifts) | 0.76 | 0.79 (0.045) |
| Average number of lineages converging to each shared adaptive peak | 2.8 | 2.8 (0.30) |
| Fraction of convergent peaks with lineages from multiple islands | 0.88 | 0.94 (0.074) |

Anoles have diversified into many more species on the larger islands (*14*, *31*). Given the number of convergent and unique adaptive peak shifts that have occurred across the Greater Antilles in anoles, the area effect hypothesis predicts that all endemic unique peaks should occur on Cuba and Hispaniola, as observed (*18*) (fig. S3). Thus, in this system, even the apparently contingent evolution of unique ecomorphologies may be, to some extent, predictable—in this case a result of the speciation-area relationship (*30*).

Gould famously argued that evolution over long time scales is "utterly unpredictable and quite unrepeatable" (*32*, p. 14) due to historical contingency. Widespread convergence among entire faunas of Greater Antillean *Anolis* refutes Gould's claim and shows that adaptation can overcome the influence of chance events on the course of evolution. Our demonstration of deterministic convergence on a macroevolutionary adaptive landscape complements studies of diversification in species numbers in showing that many features of large-scale radiations may be surprisingly predictable. A recent analysis discovered that both island diversification rate and standing species richness in Greater Antillean anoles could be predicted from island size and time since colonization (*31*). In cichlids, whether colonizing lineages will radiate in African lakes can be predicted from the intrinsic traits of the colonist and the ecological opportunities provided by the new habitat (*33*). Together, these studies suggest that the primary aspects of evolutionary radiation—adaptation and the proliferation of species—may in some cases be largely deterministic.

### References and Notes


1. S. Gavrilets, A. Vose, *Proc. Natl. Acad. Sci. U.S.A.* **102**, 18040–18045 (2005).
2. D. Schluter, *The Ecology of Adaptive Radiation* (Oxford Univ. Press, Oxford, 2000).
3. G. G. Simpson, *Tempo and Mode in Evolution* (Columbia Univ. Press, New York, 1944).
4. E. I. Svensson, R. Calsbeek, Eds., *The Adaptive Landscape in Evolutionary Biology* (Oxford Univ. Press, Oxford, 2012).
5. B. Frédérich, L. Sorenson, F. Santini, G. J. Slater, M. E. Alfaro, *Am. Nat.* **181**, 94–113 (2013).
6. R. Gillespie, *Science* **303**, 356–359 (2004).
7. T. J. Givnish, in *The Biology of Biodiversity*, M. Kato, Ed. (Springer-Verlag, Tokyo, 1999), pp. 67–90.
8. M. Muschick, A. Indermaur, W. Salzburger, *Curr. Biol.* **22**, 2362–2368 (2012).
9. M. L. J. Stiassny, A. Meyer, *Sci. Am.* **280**, 64–69 (1999).
10. K. A. Young, J. Snoeks, O. Seehausen, *PLoS ONE* **4**, e4740 (2009).
11. Past studies of convergence between species-rich radiations have been selective in scope and have not compared entire radiations. Even lineages diversifying randomly under genetic drift will generate many convergent pairs (*34*), as will radiations adapting on a labile macroevolutionary landscape (*27*). Much of the diversity unsampled by past studies may be nonconvergent, so that different radiations may share many convergent species pairs while being unexceptionally similar at the whole-radiation scale.
12. M. L. Cody, H. A. Mooney, *Annu. Rev. Ecol. Syst.* **9**, 265–321 (1978).
13. R. Kassen, *Ann. N. Y. Acad. Sci.* **1168**, 3–22 (2009).
14. J. B. Losos, *Lizards in an Evolutionary Tree: Ecology and Adaptive Radiation of Anoles* (Univ. of California Press, Berkeley, CA, 2009).
15. E. E. Williams, in *Lizard Ecology: Studies of a Model Organism*, R. B. Huey, E. R. Pianka, T. W. Schoener, Eds. (Harvard Univ. Press, Cambridge, MA, 1983), pp. 326–370.
16. J. B. Losos, T. R. Jackman, A. Larson, K. de Queiroz, L. Rodríguez-Schettino, *Science* **279**, 2115–2118 (1998).
17. D. L. Mahler, L. J. Revell, R. E. Glor, J. B. Losos, *Evolution* **64**, 2731–2745 (2010).
18. Information on materials and methods is available as supplementary material on *Science* Online.
19. L. J. Harmon *et al.*, *Evolution* **64**, 2385–2396 (2010).
20. T. Ingram, D. L. Mahler, *Methods Ecol. Evol.* **4**, 416–425 (2013).
21. M. A. Butler, A. A. King, *Am. Nat.* **164**, 683–695 (2004).
22. T. F. Hansen, *Evolution* **51**, 1341 (1997).
23. M. E. Alfaro *et al.*, *Proc. Natl. Acad. Sci. U.S.A.* **106**, 13410–13414 (2009).
24. G. H. Thomas, R. P. Freckleton, *Methods Ecol. Evol* **3**, 145–151 (2012).
25. G. L. Conte, M. E. Arnegard, C. L. Peichel, D. Schluter, *Proc. Biol. Sci.* **279**, 5039–5047 (2012).
26. G. Pinto, D. L. Mahler, L. J. Harmon, J. B. Losos, *Proc. Biol. Sci.* **275**, 2749–2757 (2008).
27. T. F. Hansen, in *The Adaptive Landscape in Evolutionary Biology*, E. Svensson, R. Calsbeek, Eds. (Oxford Univ. Press, Oxford, 2012), pp. 205–226.
28. S. Estes, S. J. Arnold, *Am. Nat.* **169**, 227–244 (2007).
29. J. C. Uyeda, T. F. Hansen, S. J. Arnold, J. Pienaar, *Proc. Natl. Acad. Sci. U.S.A.* **108**, 15908–15913 (2011).
30. Y. Kisel, T. G. Barraclough, *Am. Nat.* **175**, 316–334 (2010).
31. D. L. Rabosky, R. E. Glor, *Proc. Natl. Acad. Sci. U.S.A.* **107**, 22178–22183 (2010).
32. S. J. Gould, *Wonderful Life: The Burgess Shale and the Nature of History* (Norton, New York, 1989).
33. C. E. Wagner, L. J. Harmon, O. Seehausen, *Nature* **487**, 366–369 (2012).
34. C. T. Stayton, *J. Theor. Biol.* **252**, 1–14 (2008).


**Acknowledgments:** We thank G. Bradburd, C. Davis, L. Harmon, and F. Jenkins for discussion and advice; the National Evolutionary Synthesis Center and NSF for financial support; and three anonymous reviewers for insightful feedback. Data are archived in Dryad (http://datadryad.org, doi: 10.5061/dryad.9g182).

### Supplementary Materials

www.sciencemag.org/cgi/content/full/341/6143/292/DC1
Materials and Methods
Figs. S1 to S9
Tables S1 to S5
References (*35*–*42*)
Author Contributions

5 November 2012; accepted 5 June 2013
10.1126/science.1232392

# Predicting and Manipulating Cardiac Drug Inactivation by the Human Gut Bacterium *Eggerthella lenta*

**Henry J. Haiser,[1] David B. Gootenberg,[1] Kelly Chatman,[1] Gopal Sirasani,[2] Emily P. Balskus,[2] Peter J. Turnbaugh[1]***

Despite numerous examples of the effects of the human gastrointestinal microbiome on drug efficacy and toxicity, there is often an incomplete understanding of the underlying mechanisms. Here, we dissect the inactivation of the cardiac drug digoxin by the gut Actinobacterium *Eggerthella lenta*. Transcriptional profiling, comparative genomics, and culture-based assays revealed a cytochrome-encoding operon up-regulated by digoxin, inhibited by arginine, absent in nonmetabolizing *E. lenta* strains, and predictive of digoxin inactivation by the human gut microbiome. Pharmacokinetic studies using gnotobiotic mice revealed that dietary protein reduces the in vivo microbial metabolism of digoxin, with significant changes to drug concentration in the serum and urine. These results emphasize the importance of viewing pharmacology from the perspective of both our human and microbial genomes.

Humans are home to large and diverse microbial communities, the most abundant of which resides in the gastrointestinal tract. Recent studies have highlighted the clinical relevance of the biotransformations catalyzed by the human gut microbiome, including alterations to the bioavailability, activity, and toxicity of therapeutic drugs (*1*, *2*). Although >40 drugs are metabolized by the gut microbiome, little is known about the underlying mechanisms. This

knowledge is critical to enable the rational design of pharmaceutical or dietary interventions.

The inactivation of the cardiac drug digoxin provides a promising starting point for understanding microbial drug metabolism. Digoxin and other cardiac glycosides have been widely used for hundreds of years to treat heart failure and arrhythmias. Therapeutic effects are accomplished indirectly when inhibition of the $Na^+$- and $K^+$-dependent adenosine triphosphatase ($Na^+/K^+$ ATPase) in cardiac myocytes raises the intracellular $Ca^{2+}$ concentration (*3*). Digoxin has a narrow therapeutic range (0.5 to 2.0 ng/ml) (*3*), and some patients excrete the inactive digoxin metabolite, dihydrodigoxin, in which the lactone ring is reduced (fig. S1A) (*4*). This modification disrupts ring planarity, which is thought to shift positioning within the binding pocket of the $Na^+/K^+$ ATPase, resulting in decreased target affinity (*5*). Coadministration of broad-spectrum antibiotics increases serum digoxin (*4*), and *Eggerthella lenta* reduces digoxin in vitro (*6*). Before this work, the molecular mechanism of digoxin reduction and the factors that alter microbial drug inactivation in vivo were unknown.

We confirmed that *E. lenta* DSM2243, the type strain, reduces digoxin in vitro (*7*) and that arginine inhibits this reaction (Fig. 1A). The growth of *E. lenta* DSM2243 was stimulated by arginine supplementation (Fig. 1A and fig. S2), indicative of using the arginine dihydrolase pathway for adenosine 5′-triphosphate (ATP) (*8*). Citrulline (an intermediate upstream of ATP production) stimulated growth, whereas ornithine (an end product) did not (figs. S2 and S3).

*E. lenta* cultures were grown anaerobically in rich medium supplemented with low and high levels of arginine (0.25% and 1.25%, respectively) in the presence or absence of digoxin (10 μg/ml), and we performed RNA sequencing (RNA-Seq) on the resultant cellular biomass (figs. S4 to S6 and table S1). A two-gene operon was highly up-regulated after exposure to digoxin during exponential growth (>100-fold) (Fig. 1B and tables S2 and S3). These two genes, referred to here as the cardiac glycoside reductase (*cgr*) operon (gene labels: *cgr1* and *cgr2*), encode proteins that are homologous to bacterial cytochromes and are therefore potentially capable of using digoxin as an alternative electron acceptor. Incubation of *E. lenta* with multiple cardiac glycosides and their reduced forms revealed that the *cgr* operon is broadly responsive to compounds with an α,β-unsaturated butyrolactone ring (figs. S7 to S9 and table S5).

Digoxin induction was increased in low-arginine conditions during both its exponential and stationary phases, relative to cultures exposed to high levels of arginine (fig. S10, A and B). *cgr* induction by digoxin and the growth phase–dependent effects exerted by arginine were confirmed on independent samples using quantitative reverse transcription polymerase chain reaction (QRT-PCR) (Fig. 1C, fig. S10C, and table S4). Unlike arginine, ornithine did not repress *cgr2* expression (fig. S11). These results are consistent with the hypothesis that arginine represses *cgr* operon expression and thereby inhibits digoxin reduction.

Next, we tested three strains of *E. lenta* (DSM2243, FAA 1-3-56, and FAA 1-1-60) (*9*, *10*) for digoxin reduction; the type strain was the sole strain capable of digoxin reduction in vitro (Fig. 1D). Comparative genomics revealed that the type strain was nearly indistinguishable from the other two strains when common marker genes were used (fig. S12). Reciprocal BLASTP comparisons of all protein-coding sequences of the three fully sequenced *E. lenta* strains revealed that the type strain shared 79.4% and 90.5% of its proteome with strains FAA 1-3-56 and FAA 1-1-60, respectively (fig. S12). The *cgr* operon was unique to the type strain (table S6); furthermore, the two nonreducing *E. lenta* strains were missing three genomic loci, which were also up-regulated by digoxin, and are predicted to encode membrane transporters for the uptake of small molecules and glycosides (fig. S13). Arginine did not significantly decrease the expression level of these transporters (fig. S14).

Strain-level variation provides an explanation for the difficulties in predicting dihydrodigoxin levels in cardiac patients by the presence or ab-

[1]Faculty of Arts and Sciences (FAS) Center for Systems Biology, Harvard University, Cambridge, MA 02138, USA. [2]Department of Chemistry and Chemical Biology, Harvard University, Cambridge, MA 02138, USA.

*Corresponding author. E-mail: pturnbaugh@fas.harvard.edu (P.J.T.)

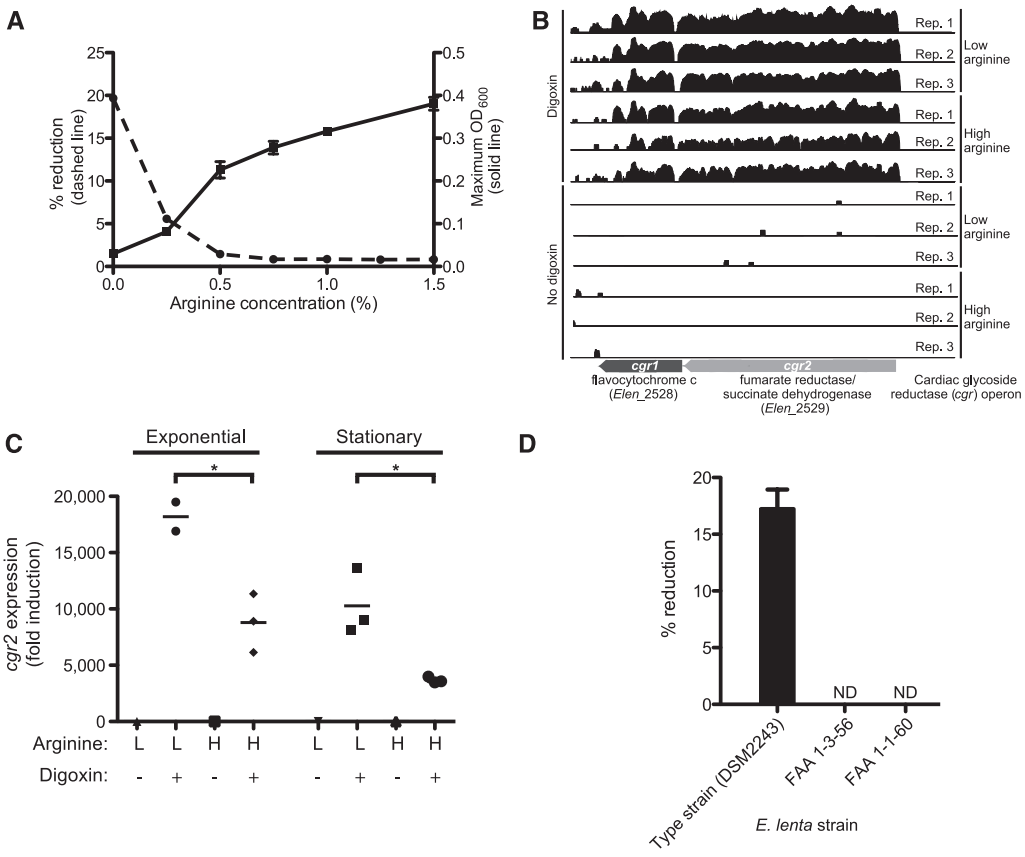


**Fig. 1. Discovery of a bacterial operon induced by digoxin.** (**A**) Arginine stimulates the growth of *E. lenta* DSM2243 in vitro while blocking the reduction of digoxin. Maximum optical density (absorbance) at 600 nm ($OD_{600}$) (solid line; values are means ± SEM; $n = 3$) and digoxin percentage reduction efficiency (dashed line; values are means; $n = 2$) after 48 hours of growth. (**B**) RNA-Seq profiles of the *cgr* operon are shown with and without digoxin during exponential growth in medium containing low or high arginine. The height is proportional to the natural log of the number of unambiguous sequencing reads mapped to each base. (**C**) *cgr2* transcription as determined by QRT-PCR. Asterisks indicate statistical significance by Student's *t* test ($P < 0.05$). Horizontal lines are means; $n = 2$ to 3. (**D**) Identification of two strains of *E. lenta* incapable of reducing digoxin. Values are means ± SEM; $n = 3$. ND, no reduction detected.

sence of *E. lenta* (*6*, *11*). We used quantitative PCR (QPCR) to measure the abundance of the *cgr* operon relative to the *E. lenta* 16*S* ribosomal RNA (rRNA) gene (the "*cgr* ratio") in microbial community DNA from 20 unrelated healthy people, along with ex vivo digoxin reduction assays. The results stratified our cohort into low reducers (12.82 ± 10.68% reduction; $n = 6$) and high reducers (96.25 ± 7.69% reduction; $n = 14$) (Fig. 2A). The *cgr* ratio was significantly increased for the high reducers (1.058 ± 0.562) when compared with low reducers (0.425 ± 0.582; $P < 0.05$, Student's $t$ test) (Fig. 2B and fig. S15). Linear regression of reduction efficiency with the *cgr* ratio revealed a significant correlation ($R^2 = 0.22$, $P < 0.05$), whereas the abundance of *E. lenta* failed to predict the extent of reduction ($R^2 = 0.06$, $P = 0.30$). The optimal *cgr* ratio cutoff (0.6) predicted digoxin reduction efficiency with a sensitivity of 86%, specificity of 83%, and precision of 92%.

Coculture of *E. lenta* with the fecal microbiome enhanced the efficiency of digoxin reduction. Each low-reducing fecal sample was incubated with the type (reducing) and FAA 1-3-56 (nonreducing) strains of *E. lenta*. The communities incubated with the type strain reduced more digoxin (95.39 ± 2.41%) than the type strain alone (68.91 ± 7.70%; $P < 0.05$, Mann-Whitney $U$ test) (Fig. 2C). The *cgr* ratio was significantly elevated after coculture (Fig. 2D) and was tightly linked to reduction efficiency ($R^2 = 0.74$, $P < 0.0001$). An explanation for the observed microbial synergy is that the fastidious growth of *E. lenta* is promoted by growth factors supplied by the gut microbiota, a phenomena that is known to affect the metabolism of environmental pollutants by soil microbial communities (*12*), along with competition for arginine that boosts digoxin reduction by *E. lenta*. Consistent with these hypotheses, the abundance of the *E. lenta* type strain was significantly increased in the presence of a complex microbial community (1.6e6 ± 4.8e5 versus 1.8e5 ± 8.4e3 in isolation; $P < 0.05$, Mann-Whitney test), and arginine supplementation suppressed the reduction of digoxin during coculture (fig. S16).

Diet could also explain interindividual variations in digoxin reduction. In vitro growth of *E. lenta* showed that, although arginine stimulated cell growth, it decreased *cgr* operon expression and prevented the conversion of digoxin to dihydrodigoxin (Fig. 1, A and C, and fig. S10). These observations led us to hypothesize that increased consumption of dietary protein, and the corresponding increase in arginine, would inhibit the in vivo reduction of digoxin by *E. lenta*. Germ-free adult male Swiss-Webster mice were colonized with the type strain before being fed diets differing only in the amount of total protein ($n = 5$ mice/group) (tables S7 and S8 and fig. S17A). *E. lenta* colonized mice fed both diets (fig. S18A) and exhibited high levels of expression of the *cgr* operon (fig. S18B). Quantification of serum and urine digoxin (*7*) revealed significant increases in mice fed the high-protein diet, indicative of suppressed digoxin reduction by *E. lenta* (Fig. 3, A and B). These trends were also consistent with fecal analysis of samples from each group of mice 4 to 16 hours after digoxin administration (Fig. 3). We also confirmed that the high-protein diet significantly elevated the amino acids in the distal small intestine (*7*), which resulted in a fold increase of 1.71 ± 0.06 ($P < 0.001$, Wilcoxon test) (tables S9 and 10).

We controlled for the indirect effects of host diet and colonization that might alter digoxin pharmacokinetics irrespective of reduction by *E. lenta*. Germ-free mice were colonized with either the digoxin-reducing type strain or the nonreducing FAA 1-3-56 strain and subsequently fed the same two diets (fig. S17B). As seen before, we detected colonization with both strains, high–*cgr* operon expression, and elevated serum and urine digoxin on the high-protein diet for mice colonized with the type strain (Fig. 3, C and D, and fig. S18, C and D). Diet did not significantly affect the serum or urine digoxin levels of mice colonized with the nonreducing strain (Fig. 3, C and D). Serum digoxin was significantly lower in mice colonized with the type strain fed the 0% protein diet, relative to those colonized with the nonreducing strain (4.91 ± 1.56 ng/ml vs.

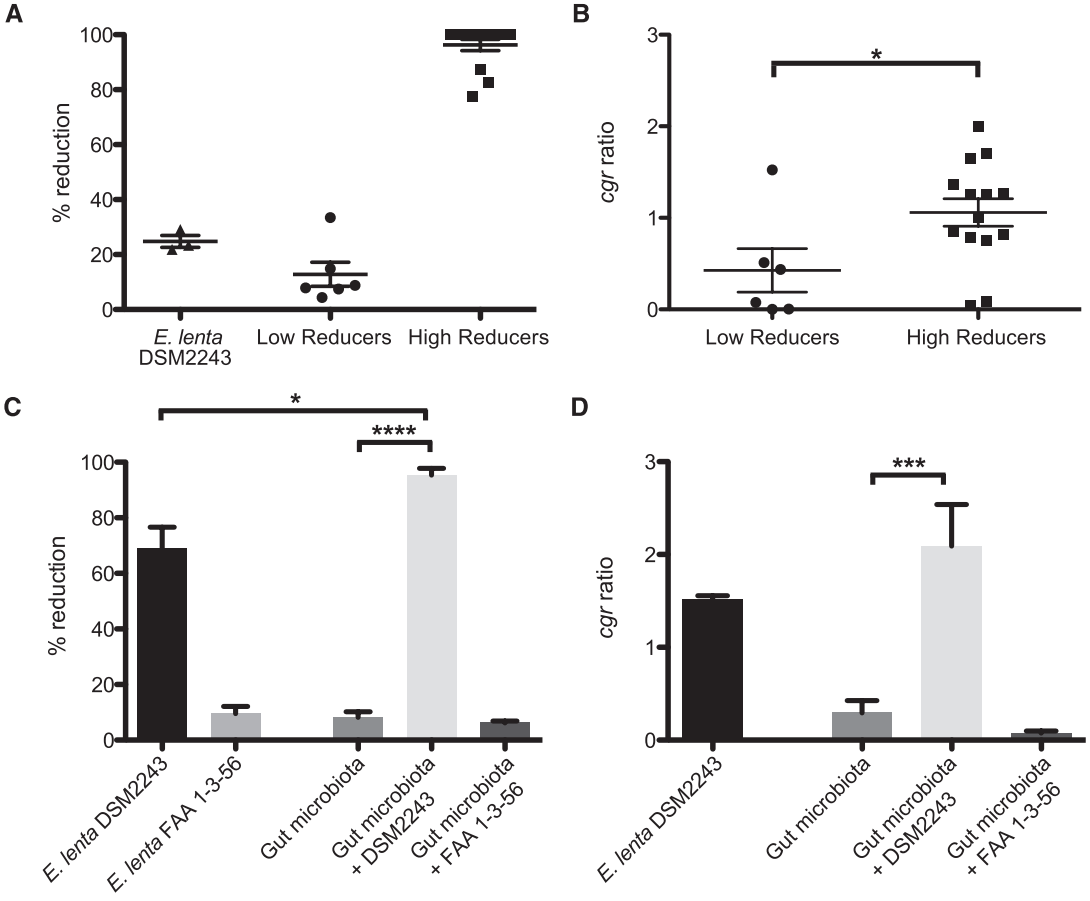


**Fig. 2. A microbial biomarker predicts the inactivation of digoxin.** (**A**) Liquid chromatography–mass spectrometry (LC-MS) was used to quantify digoxin reduction in the fecal microbiomes of 20 unrelated individuals. (**B**) The *cgr* ratio was significantly different between low and high reducers. Data represent QPCR with the *cgr2* gene, and *E. lenta*–specific 16*S* rDNA primers (table S4). (**C**) Five low-reducing fecal microbial communities were incubated for 5 days in the presence or absence of *E. lenta* DSM2243 or FAA 1-3-56. LC-MS was used to quantify the completion of digoxin reduction. Supplementation with the nonreducing strain of *E. lenta* did not significantly affect digoxin reduction efficiency. (**D**) The *cgr* ratio was obtained for each of the low-reducing microbial communities after incubation. Outliers were identified using Grubbs' test ($P < 0.01$) and removed. Values are means ± SEM. Points in (A) and (B) represent biological replicates. Asterisks indicate statistical significance by Student's $t$ test (*$P < 0.05$; ***$P < 0.001$; ****$P < 0.0001$).

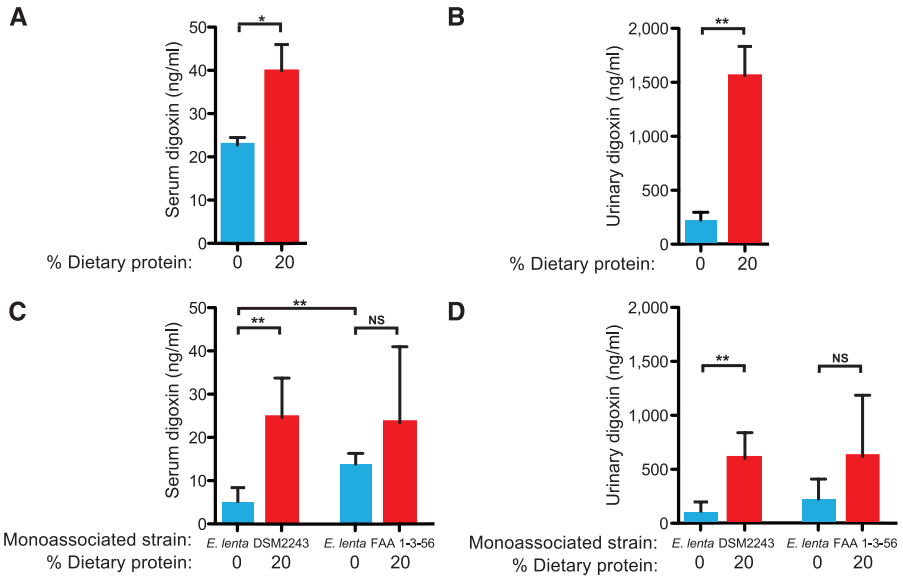


**Fig. 3. Dietary protein blocks the inactivation of digoxin.** Serum (**A**) and urinary (**B**) digoxin levels from the type strain experiment. Fecal digoxin levels showed a consistent trend: the mean area under the curve was 6.226 ng digoxin per hour per ml in germ-free mice, 3.576 for mice fed the 0% protein diet, and 6.364 for mice fed the 20% protein diet. Serum (**C**) and urinary (**D**) digoxin levels from each group. Digoxin levels were quantified by enzyme-linked immunosorbent assay (ELISA) (*7*). Values are means ± SEM. Asterisks indicate statistical significance by Student's *t* test (*$P < 0.05$; **$P < 0.01$). $n = 4$ to 5 mice per group. NS, not significant.

13.8 ± 1.25; $P < 0.01$, Student's *t* test) (Fig. 3C). Together, these results suggest that the enhanced free amino acids available to *E. lenta* inhibited the activity of the *cgr* operon and increased the bioavailability of digoxin.

An expanded model of digoxin pharmacokinetics is now emerging: Colonization by distinct strains of *E. lenta,* microbial interactions, and host diet act together to influence drug levels (fig. S19). Follow-up studies in cardiac patients are necessary to determine whether rapid QPCR-based biomarker assessments of the gut microbiome can guide dosage regimes. It may also be possible to provide dietary guidelines or supplements that prevent microbial drug metabolism. More broadly, our results emphasize that a comprehensive view of pharmacology includes the structure and activity of our resident microbial communities and a deeper understanding of their interactions with each other, with their host habitat, and with the nutritional milieu of the gastrointestinal tract.

## References and Notes


1. H. J. Haiser, P. J. Turnbaugh, *Science* **336**, 1253–1255 (2012).
2. B. D. Wallace *et al.*, *Science* **330**, 831–835 (2010).
3. L. S. Goodman *et al.*, *Goodman & Gilman's the Pharmacological Basis of Therapeutics* (McGraw-Hill, New York, ed. 12, 2011).
4. J. Lindenbaum, D. G. Rund, V. P. Butler Jr., D. Tse-Eng J. R. Saha, *N. Engl. J. Med.* **305**, 789–794 (1981).
5. C. D. Farr *et al.*, *Biochemistry* **41**, 1137–1148 (2002).
6. J. F. Dobkin, J. R. Saha, V. P. Butler Jr., H. C. Neu, J. Lindenbaum, *Science* **220**, 325–327 (1983).
7. Materials and methods are available as supplementary materials on *Science* Online.
8. J. F. Sperry, T. D. Wilkins, *J. Bacteriol.* **127**, 780–784 (1976).
9. E. Saunders *et al.*, *Stand. Genomic Sci.* **1**, 174–182 (2009).
10. K. E. Nelson *et al.*, *Science* **328**, 994–999 (2010).
11. V. I. Mathan, J. Wiederman, J. F. Dobkin, J. Lindenbaum, *Gut* **30**, 971–977 (1989).
12. X. Maymó-Gatell, Y. Chien, J. M. Gossett, S. H. Zinder, *Science* **276**, 1568–1571 (1997).



**Acknowledgments:** B. Budnik and S. Trauger for liquid chromatography–mass spectrometry (LC-MS) analyses; V. Yeliseyev, A. Liou, and R. Carmody for mouse studies; C. Reardon and C. Daly for sequencing support; C. Maurice, L. David, R. Dutton, B. Wolfe, J. Button, M. Elliot, Y. Falanga, R. Losick, A. Murray, and B. Stern for helpful discussions. Mouse experiments were done with the generous support of the Harvard Digestive Diseases Center and the University of North Carolina gnotobiotic cores. This work was supported by grants from the NIH (P50 GM068763) and the Harvard Digestive Diseases Center (2P30DK034854-26). H.J.H. is supported by the Canadian Institutes of Health Research (MFE-112991). RNA-Seq data are deposited in the Gene Expression Omnibus (GEO) database (accession GSE43919).


## Supplementary Materials

www.sciencemag.org/cgi/content/full/341/6143/295/DC1
Materials and Methods
Figs. S1 to S19
Tables S1 to S10
References (*13*–*25*)


30 January 2013; accepted 14 June 2013
10.1126/science.1235872

Science
AAAS

# Predicting and Manipulating Cardiac Drug Inactivation by the Human Gut Bacterium *Eggerthella lenta*

Henry J. Haiser *et al.*

*Science* **341**, 295 (2013);
DOI: 10.1126/science.1235872



*Science* (print ISSN 0036-8075; online ISSN 1095-9203) is published weekly, except the last week in December, by the American Association for the Advancement of Science, 1200 New York Avenue NW, Washington, DC 20005. 